*J. Chem. Sci.* (2022)134:51
https://doi.org/10.1007/s12039-022-02045-1


**REGULAR ARTICLE**

# Why do some reactions possess similar reaction rate in wildly different viscous media? A possible explanation *via* frequency-dependent friction

ATANU BAKSI and RANJIT BISWAS*
Department of Chemical, Biological and Macromolecular Sciences, S. N. Bose National Centre for Basic Sciences, JD Block, Sector-III, Salt Lake, Kolkata 700106, India
E-mail: ranjit@bose.res.in

MS received 10 December 2021; revised 16 February 2022; accepted 16 February 2022

**Abstract.** We explore herein the interconnection between the collective intermolecular solvent modes (CIM) and ultrafast reaction rate, assuming that frequency-dependent solvent friction controls the rate of such reactions. We attempt to find a possible explanation for the observed near-insensitivity of ultrafast reaction rates (for example, charge transfer reaction) to the medium viscosity. Results are presented here by employing an analytical scheme that estimates the high-frequency solvent frictional response. Representative room temperature reaction media considered here are an ionic liquid ($BMIMPF_6$, $\eta \sim 310$cP), a dipolar solvent (ethanol, $\eta \sim 1.09$cP) and a deep eutectic solvent (Acetamide+ LiBr, $\eta \sim 1950$cP). It is found that the wavenumber and frequency-dependent rotational friction, $\Gamma_R(\kappa, z)$, estimated by using the available experimental dielectric relaxation (DR) data for the ionic liquid and the deep eutectic solvent (DES), cannot predict the viscosity independence of $\Gamma_R(\kappa, z)$ at high frequency. Missing dispersion in the DR data of the DES appears to be critical and incorporation of this missing amplitude via collective solvent intermolecular modes centered around 100 $cm^{-1}$ markedly improves the high-frequency behaviour of $\Gamma_R(\kappa, z)$. Subsequently, the calculated $\Gamma_R(\kappa, z)$ for these solvents at high frequency exhibits near-insensitivity to medium viscosity and explain the viscosity independence of ultrafast reaction rates.

**Keywords.** Ultrafast reaction; viscosity dependence; frequency-dependent friction; collective intermolecular solvent modes (CIM).

## 1. Introduction

This paper explores the interconnection between solvent friction and reaction rate. This is one of the ways that a solvent can exert control on a reaction occurring in it. Solvent polarity is the other factor that can tune a reaction *via* modifying the reaction barrier.[1,2] In a two-dimensional picture of a reaction barrier separating the reactant and the product surfaces, a reactant molecule experiences solvent friction while crossing the barrier top. The downward curvature of the barrier then decides the extent of coupling between the reaction rate and solvent friction. In a non-Markovian rate theory,[3,4] the friction experienced by the reactant is not that exerted by the zero frequency shear viscosity of the medium. The frictional resistance, in contrast, depends on the frequency with which the reactive mode vibrates and/or oscillates. This, in other words, sets a timescale for the reactant to reside on the barrier top. If the barrier is high and the curvature is sharp, the medium friction becomes the friction that involves the faster collective modes of the solvent motion. For a low barrier reaction, relatively broadened curvature allows the reactant to spend more time on the barrier top, probing solvent friction for a longer duration. Reactions involving low barrier are therefore amenable to frictional resistance proportional to medium viscosity and the solvent impact on these reactions can be understood *via* the Smoluchowski description[5,6] of the reaction in the overdamped limit. For barrier-less reactions, on the other hand, solvent control may arise from the stabilization of the intermediate or the newly

*For correspondence
*Supplementary Information: The online version contains supplementary material available at https://doi.org/10.1007/s12039-022-02045-1.*

Published online: 01 April 2022

germinated product molecule where underdamped solvent modes such as collective intermolecular modes (CIM) and librations assume significant importance.

For ultrafast reactions, such as electron transfer reactions (ETRs), collective solvent modes can indeed be critically important. This is probably reflected in the repeated observation of ETRs and charge transfer reactions (CTRs) being nearly insensitive to or strongly decoupled from solvent viscosity.[7–9] This can be qualitatively explained by either assuming that solvents play a minimal role for these CTRs or only the ultrafast solvent polarization modes couple to these reactions. ETRs involve appreciable charge transfer (for example, $Fe^{+2} \rightarrow Fe^{+3}$) and it is difficult to believe that solvent polarization can remain non-responsive to such charge transfer and the subsequent stabilization *via* solvent reorganization. One approach then would be to explore that part of the solvent friction which involves inertial and collective solvent modes. This, in turn, means the calculations of the frequency-dependent solvent friction, incorporating both the collective and diffusive solvent modes consistently. Fortunately, such a prescription is already available.[10–13] In this scheme, the generalized rate of solvent polarization contains the wavenumber ($k$) and frequency ($z$) dependent solvent rotational ($\Gamma_R(k,z)$) and translational ($\Gamma_T(k,z)$) frictional kernels. The $k \rightarrow 0$ and $z \rightarrow \infty$ limits of these kernels then describe the frictional response arising from the collective and inertial solvent modes. In the collective wavenumber limit ($k \rightarrow 0$), $\Gamma_R(k \rightarrow 0, z)$ has been connected to the frequency-dependent dielectric function, $\varepsilon(z)$, of a medium that can be accessed *via* dielectric relaxation (DR) measurements. Note here that in this wavenumber limit, extremely fast underdamped solvent motions fall in the high-frequency regime and have been incorporated *via* the intermolecular vibrations and librations that contribute to the dielectric dispersion from the infinite frequency dielectric constant to the square of the refractive index, $\varepsilon_\infty - n^2$. In DR experiments, this normally belongs to the tera-Hertz regime of $\varepsilon(z)$.

Three differently viscous media spanning a viscosity variation of three orders of magnitude have been considered for generating representative results here. They are a room temperature ionic liquid ([BMIM][$PF_6$], $\eta \sim 310$cP),[14] a common dipolar solvent (ethanol, $\eta \sim 1.08$cP)[15] and an ionic deep eutectic solvent (Acetamide + LiBr, $\eta \sim 1950$cP).[16] Calculations have been performed at or near room temperature. Please see Table 1. Rotational frictional kernel ($\Gamma_R(k,z)$) has been calculated, as already mentioned, by using the analytical expression that connects solvent medium friction to the experimental dielectric relaxation (DR) data.[10]

## 2. Theoretical Formalism and Method of Calculation

The relation that connects the wavenumber and frequency-dependent rotational frictional kernel, $\Gamma_R(k,z)$, to the frequency-dependent dielectric function, $\varepsilon(z)$, is the following:[17–19]

$$\frac{2k_BT}{I[z+\Gamma_R(k,z)]} = \frac{z\varepsilon_0[\varepsilon(z)-\varepsilon_\infty]}{f(110;k\rightarrow 0)\varepsilon_\infty[\varepsilon_0-\varepsilon_\infty]}, \quad (1)$$

where, $\varepsilon_\infty$ is the dielectric constant in the high-frequency limit and $I$ the moment of inertia. $f(110,k)$ is related to the orientational direct correlation function, $c(100,k)$, through the relation[20,21] $f(110,k) = 1 - (\rho_d^0/4\pi)\, c(110,k)$.

The necessary inputs for the calculations of $\Gamma_R(k,z)$ are therefore as follows: (i) the wavenumber dependent orientational static structure factor, $c(110,k)$ and (ii) the experimental dielectric relaxation data of these liquids. The orientational static structure factor for these liquids is obtained from the mean spherical approximation (MSA) model[22,23] with proper correction at $k \rightarrow 0$, using the experimental static dielectric constant after assuming the dipolar species as dipolar hard spheres.

The dielectric relaxation data used in the present calculations have been taken from various measurements employing different frequency windows: $(0.1 \le \nu/GHz \le 3000)$ for [BMIM][$PF_6$],[24] $(0.2 \le \nu/GHz \le 50)$ for the ionic DES,[16] $(0.2 \le \nu/GHz \le 89)$ for ethanol.[25] In those DR experiments, measured $\varepsilon(z)$ data were found to fit to the following forms,

$$\varepsilon(\nu) = \varepsilon_\infty + \frac{\Delta\varepsilon_1}{(1+(i2\pi\nu\tau_1)^{1-\alpha_1})^{\beta_1}} + \frac{\Delta\varepsilon_2}{(1+i2\pi\nu\tau_2)} + \frac{\Delta\varepsilon_3}{(1+i2\pi\nu\tau_3)} + \frac{\Delta\varepsilon_4}{{\nu_4}^2-\nu^2+i\gamma_4\nu},$$

for [BMIM][$PF_6$],

$$\varepsilon(\nu) = \varepsilon_\infty + \sum_{j=1}^{j=4}\frac{\Delta\varepsilon_j}{(1+i2\pi\nu\tau_j)}, \quad \text{for (acetamide + LiBr) DES},$$

$$\varepsilon(\nu) = \varepsilon_\infty + \sum_{j=1}^{j=3}\frac{\Delta\varepsilon_j}{(1+i2\pi\nu\tau_j)}, \quad \text{for ethanol.}$$

**Table 1.** Viscosity values and dielectric constants for the DES, [BMIM][PF6] and ethanol.

| System | Acetamide + LiBr (DES) | [BMIM][PF6] (IL) | Ethanol (dipolar liquid) |
|---|---|---|---|
| Viscosity (cP) | 1950 (293 K) | 310 (298 K) | 1.095 (298 K) |
| $\varepsilon_0$ | 23.6 (293 K) | 11.8 (298 K) | 24.35 (298 K) |

Here $\tau_j$ denotes the relaxation time associated with the $\Delta\varepsilon_j$ dispersion. $\alpha_1$ and $\beta_1$ determine the shape of a relaxation mode. In addition, $z = 2\pi iv$. The experimental dielectric relaxation data for these three systems are provided in Table 2.

The orientational dynamics is calculated through the following prescription.[10,14,18–21,26,27] We have calculated the reorientation time correlation function (RTCF) of rank $\ell$ by Laplace transformation ($\mathcal{L}^{-1}$) of a frequency dependent term which is dependent on rotational kernel found from equation 1. Laplace transform is then numerically obtained *via* the Stehfest algorithm.

$$C_\ell(t) = \mathcal{L}^{-1}\left\{z + \frac{\ell(\ell+1)k_BT}{I[z+\Gamma_R(z)]}\right\}^{-1} \tag{2}$$

RTCFs for $\ell = 1$ have been calculated from equation 2. Multi-exponential fits to the simulated RTCFs then lead to the analytical estimation of the average reorientational correlation times through time integration: $\tau^{\ell}_{avg} = \int_0^\infty dt C_\ell(t) = \frac{\sum a_i\tau_i}{\sum a_i}$.

It is evident from Table 3 that a considerable part of the high frequency dispersion, $\varepsilon_\infty - {n_D}^2$, has remained undetected in the present measurements for (Acetamide +LiBr) DES. This means that the relevant calculations have completely missed the frictional contributions from the ultrafast solvent modes.

In order to account for the missing high frequency dielectric dispersion in our calculations, we have attributed this dispersion, $\varepsilon_\infty - {n_D}^2$, to one or a couple of damped collective intermolecular modes of the solvent as follows:[12–14,24,28]

$$\varepsilon(z) = \varepsilon_\infty + \sum_i \frac{\Delta S_i}{[1+(z\tau_i)^{1-\alpha_i}]^{\beta_i}} + [\Delta S_{CIM}\Omega^2/(\Omega^2 + z^2 + z\Gamma)] \tag{3}$$

where $\Gamma$, the damping constant, being approximately twice as large as the resonating frequency $\Omega$, and $\Delta S_{CIM} = \varepsilon_\infty - {n_D}^2$. We expect a little variation in $\Omega$ will not affect the qualitative understanding regarding the role of this collective mode in the high frequency frictional response of the medium. This assignment is similar in spirit to what was done before while calculating ionic conductivities and dynamic solvation response in water.[10]

Measurements[24] of $\varepsilon(z)$ in the frequency range of $0.1 \leq z/GHz \leq 3000$ have indicated contributions from the IL collective modes around $\sim$70-120 $cm^{-1}$ for several imidazolium ILs. This has been assigned to cation CIM (restricted rotation or oscillatory motion). Terahertz time-domain spectroscopic measurements[29] involving metalocenium ILs have suggested that interion vibrations between the cations and anions and cation CIM are responsible for the observed dynamics in the THz region. These studies have also revealed that the bands appearing in the frequency range $\sim$ 20–50 $cm^{-1}$ show the maximum amplitude. Optical heterodyne-detected Raman-induced Kerr-effect

**Table 2.** Experimental DR data for [BMIM][PF6], DES, and ethanol.

| System | $\varepsilon_0$ | $\tau_1$ | $\alpha_1$ $\beta_1$ | $\Delta\varepsilon_1$ | $\tau_2$ | $\Delta\varepsilon_2$ | $\tau_3$ | $\Delta\varepsilon_3$ | $\tau_4$ | $\Delta\varepsilon_4$ | $\varepsilon_\infty$ |
|---|---|---|---|---|---|---|---|---|---|---|---|
| [BMIM][$PF_6$] | 11.8 | 1406 | 0.0<br>0.37 | 7.04 | 38.8 | 0.45 | 1.26 | 0.81 | $\nu_4$= 2.77 THz<br>$\gamma_4$= 7.77 THz | 1.38 | 2.10 |
| Acetamide + LiBr | 23.6 | 715 | | 13.3 | 131 | 3.0 | 30 | 1.4 | 4.0 | 0.4 | 5.6 |
| Ethanol | 24.3 | 161 | | 20.2 | 3.3 | 1.43 | 1.43 | 0.22 | | | 1.93 |

**Table 3.** Missing dispersion and frequency coverage of different experiments.

| System | $\varepsilon_0$ | $\varepsilon_\infty$ | ${n_D}^2$ | $\varepsilon_\infty - {n_D}^2$ | Frequency window (employed in experiments) |
|---|---|---|---|---|---|
| [BMIM][$PF_6$] | 11.8 | 2.10 | 1.9850 | 0.115 (1.18%) | 0.1 GHz–3 THz[24] |
| (Acetamide + LiBr) | 23.6 | 5.6 | 1.9796 | 3.62 (20.11%) | 0.2 GHz–50 GHz[16] |
| Ethanol | 24.35 | 1.93 | 1.85 | 0.09 (0.4%) | 0.1 GHz–1.5 THz[25] |

spectroscopic (OHD-RIKES) study[30–35] of several imidazolium ILs have attributed the collective IL dynamics in this region to the collective intermolecular modes of imidazolium ring at frequencies at 30, 65 and 100 $cm^{-1}$ corresponding to different anionic configuration around cations. Interestingly, simulation studies[36–38] with a finite number of cations and anions (within ILs) have also suggested the collective dynamics in the THz region ($\sim$30 $cm^{-1}$).

In the low frequency Kerr spectra[39] for DESs obtained *via* Fourier transforming the collected Kerr transients, a characteristic band clearly appears for $[0.78CH_3CONH_2 + 0.22LiBr]$ DES. Because of less depolarized Raman activities of intermolecular/interionic vibrational motions for spherical ions (which are mostly collision induced or interaction induced translational motions), this band can only be attributed to the collective solvent mode involving the H-bonded molecules. This has motivated us to assign the resonating frequency at around $100cm^{-1}(\sim 3THz)$ for this DES for carrying out the dispersion, $\varepsilon_\infty - {n_D}^2$, unaccounted for in the available DR data.

## 3. Numerical Results and Discussion

### 3.1 *Frequency-dependent rotational kernel, $\Gamma_R(k \to 0, z)$ employing experimental DR data*

Frequency-dependent rotational frictional kernel, $\Gamma_R(k, z)$, calculated *via* equation 1 in the limit of zero wavenumber, is presented in Figure 1 for the three representative solvents. Available experimental DR data[16,24,25] from The dielectric relaxation data used in the present calculations have been taken from various measurements employing different frequency windows: $(0.1 \le \nu/\mathrm{GHz} \le 3000)$ for [BMIM][$PF_6$],[24] $(0.2 \le \nu/\mathrm{GHz} \le 50)$ for the ionic DES,[16] $(0.2 \le \nu/\mathrm{GHz} \le 89)$ for ethanol.[25] In those DR experiments, measured $\varepsilon(z)$ data were found to fit to the following forms,

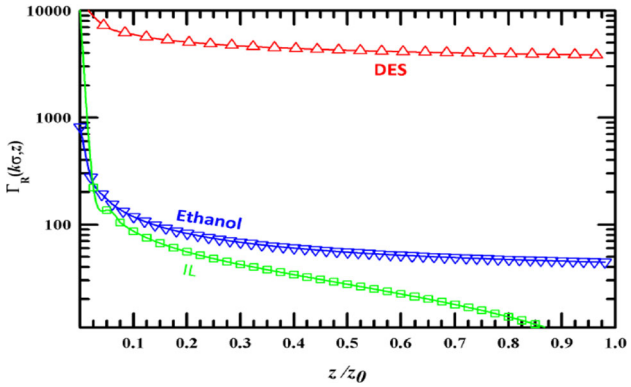


**Figure 1.** Frequency dependent rotational frictional kernel, $\Gamma_R(k\sigma \to 0, z)$, for the three different systems obtained via using the experimentally available dielectric relaxation (DR) data. Note the frequency axis has been scaled with the highest frequencies accessed. $z_0$ being the highest frequency at which experimental DR data is available for corresponding systems (see Table 3).

$$\varepsilon(\nu) = \varepsilon_\infty + \frac{\Delta\varepsilon_1}{(1 + (i2\pi\nu\tau_1)^{1-\alpha_1})^{\beta_1}} + \frac{\Delta\varepsilon_2}{(1 + i2\pi\nu\tau_2)} + \frac{\Delta\varepsilon_3}{(1 + i2\pi\nu\tau_3)} + \frac{\Delta\varepsilon_4}{\nu_4^2 - \nu^2 + i\gamma_4\nu},$$

for [BMIM][$PF_6$],

$$\varepsilon(\nu) = \varepsilon_\infty + \sum_{j=1}^{j=4} \frac{\Delta\varepsilon_j}{(1 + i2\pi\nu\tau_j)}, \text{ for (acetamide + LiBr) DES,}$$

$$\varepsilon(\nu) = \varepsilon_\infty + \sum_{j=1}^{j=3} \frac{\Delta\varepsilon_j}{(1 + i2\pi\nu\tau_j)}, \text{ for ethanol.}$$

Here $\tau_j$ denotes the relaxation time associated with the $\Delta\varepsilon_j$ dispersion. $\alpha_1$ and $\beta_1$ determine the shape of a relaxation mode. In addition, $z = 2\pi i\nu$. The experimental dielectric relaxation data for these three systems are provided in Table 2.

Table 2 has been used in these calculations as inputs. Note the available frequency coverage of all three systems is not the same. The frequency (horizontal axis) has been scaled with the highest frequency coverage $(z_0)$ of DR data of each individual systems. Note, for Ionic Liquid $z_0$ is 3 THz, for DES $z_0$ is 50 GHz whereas for Ethanol $z_0$ is 1.5 THz. For example, for DES, frequency has been scaled with 50 GHz – the highest frequency of the measurement window. We find that at the high-frequency region rotational kernel of three different system approaches three different values, the difference being huge between the DES and the other two solvents.

It is now important to note that a significant amount of dispersion is missing in the DR data summarized in Table 3. The most pronounced missing dispersion ($\sim$20% of the total available dispersion) is for the DES studied here where the frequency window employed in the measurements was $0.2 \leq \nu/GHz \leq 50$. For IL and ethanol, the missing components are relatively smaller, $\sim$1.2% and $\sim$0.4%, respectively. This is the reason for the dramatic difference in $\Gamma_R(k \to 0, z)$ between the DES and the other two solvents.

In order to address this issue, we have attributed the missing dispersion, as discussed earlier in section 2, to a CIM centered at 100cm$^{-1}$ for all these three systems, and calculated $\Gamma_R(k \to 0, z)$. The rotational kernel for these three systems after the addition of CIM mode are depicted in Figure 2. One can of course ascribe the missing dispersion to multiple bands with frequencies between 30 and 100 cm$^{-1}$ but the qualitative character of $\Gamma_R(k \to 0, z)$ at high frequency will not undergo a drastic change. Numerical results after incorporating the missing high-frequency dispersion are shown in Table 4. The inseparability of the calculated frictional kernels, particularly at higher frequencies, is quite insightful. The near independence and/or strong decoupling of CTRs on solvent viscosity can now be explained in terms of nearly the same solvent rotational frictional response at high frequency in these three solvents of widely different viscosities. It is also interesting to note that, although the zero-frequency rotational friction $(\Gamma_R(0))$ for these three systems are drastically different from each other (because it probes the zero-frequency dielectric constant, $\varepsilon_0$), the high frequency rotational response $(\Gamma_R(\infty))$ is quite small compared to the zero-frequency value and comparable to each other. Numerical values corresponding to zero-frequency rotational friction $(\Gamma_R(0))$ and the high frequency rotational response $(\Gamma_R(\infty))$ are summarized in Table 4.

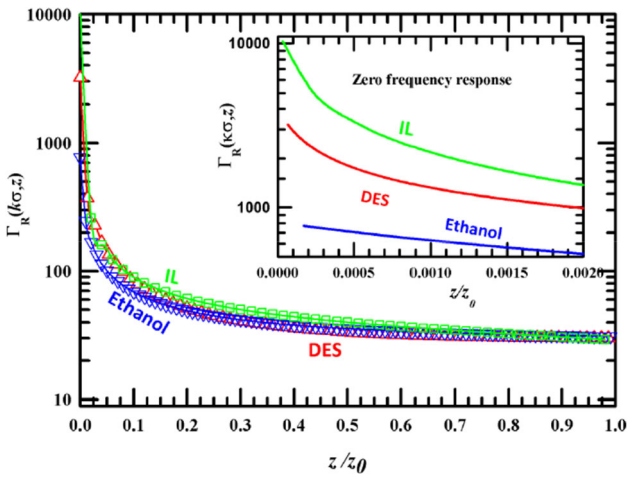


**Figure 2.** Frequency-dependent rotational Kernel for three different systems obtained after addition of an ultrafast component to experimentally available dielectric relaxation (DR) data. X-axis has been scaled with $z_0 =$ 3THz for all the systems.

### 3.2 *Reorientational time correlation function of rank $\ell = 1$, $C_1(t)$: roles of collective solvent intermolecular modes*

Next, we examine how the addition of collective intermolecular modes influences analytically evaluated reorientational timescales of these three systems and leads to better agreement between theory and simulations. Reorientational time correlation function RTCF of rank $\ell$, $C_\ell(t)$ has been calculated *via* equation 2. First, we have used experimentally available DR data as input to equation 2 and calculated $C_1(t)$. We present the numerical results in Figure S1. These $C_1(t)$ decays have been found to fit multi-exponential functions of time.

Next, following our earlier approach we have incorporated collective intermolecular mode (CIM) at a resonating frequency of 100 $cm^{-1}$ for the missing dielectric dispersion at high frequency. With these modified DR data for these three solvents $C_1(t)$ decays have been calculated. Results are shown in Figure 3.

The comparison of the average rotational timescale between analytical calculation and simulations are

**Table 4.** Zero frequency and high-frequency rotational Kernel values for three systems [BMIM][PF6], DES, and Ethanol.

| System | $\Gamma_R(0)$ | $\Gamma_R(\infty)$ |
|---|---|---|
| IL ([BMIM][$PF_6$]) | 10,000 | 29 |
| DES (Acetamide + LiBr) | 3206 | 30 |
| Ethanol | 169 | 30 |

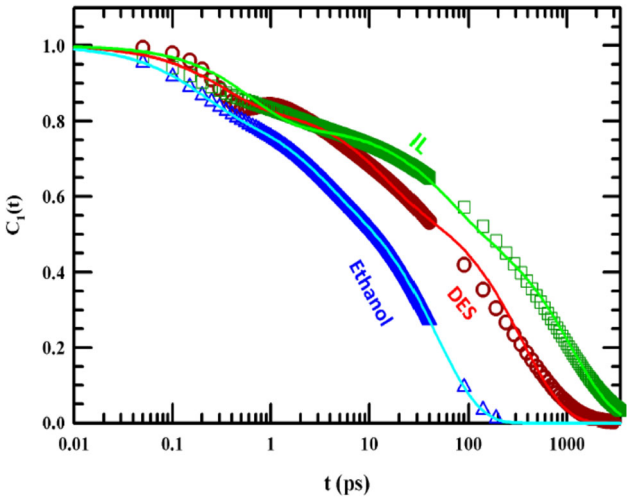


**Figure 3.** RTCF of rank $\ell$=1 for [BMIM][PF6], DES, and ethanol obtained *via* equation 2 after addition of CIM at 100 $cm^{-1}$ to the experimentally available DR data as input.

provided in Table 5 for these three systems studied here. The multi-exponential fit parameters corresponding to $C_1(t)$ with and without ultrafast component along with available simulated parameters are presented in Tables S1-S3 (Supplementary Information).

Data in Table S1 (SI) suggest that reorientation time predicted from our analytical study after addition of CIM for the ionic DES agrees better with the available simulation prediction.

Table S2 (SI) reports the multi-exponential fit parameter for [BMIM][$PF_6$] where missing dispersion was comparatively smaller ($\sim$1.2%). The analytically predicted timescales with and without the CIM contribution to experimental DR data are similar because of the small missing dispersion. The prediction of a nanosecond component ($\sim$2ns) in simulations can also be seen in our analytical calculations ($\sim$1ns). However, the 40 ns component found in simulations is completely absent. This inconsistency between theory and simulations may arise because of the following reasons: (i) 40 ns timescale corresponds to a peak frequency in the mega-Hertz (MHz) regime which has not been covered in the relevant DR measurements. Slow rotation of a composite body may account for this relaxation timescale; and (ii) the interaction potential employed for simulations of the IL may not be appropriate and therefore, this timescale might be spurious.

Table S3 (SI) summarizes the calculated and simulated timescales associated with $C_1(t)$ decay for ethanol. The analytically predicted timescales with and without the addition of the CIM contribution are also found not to be very different because of the small missing dispersion. Note that a better agreement appears between theory and simulations when the CIM contribution is incorporated in the calculations.

It is to be noted that the three systems studied here have very different polarities. In this analytical work, the wavenumber dependent dipolar static orientational correlations have been obtained by using the mean spherical approximation (MSA) where each system has been considered as a sphere with the assigned diameter and a point dipole at the center. Here we discuss about the polarity dependence of the electron transfer reaction rate in these three highly polar systems.

It has been found[43–45] that the simulated reorganization energy ($\lambda_s$) for a dipolar spherical solute lies between two continuum model-based predictions, namely, those for the van der Waals (vdW) and the solvent accessible (SA) cavities. For SA, the reorganization energy $\lambda_s \propto \frac{\varepsilon_s - 1}{2\varepsilon_s - 1}$ and for vdW $\lambda_s \propto c_0$ with the Pekar factor $c_0 = 1/\varepsilon_\infty - 1/\varepsilon_s$. $\varepsilon_\infty$ and $\varepsilon_s$ denote the high-frequency and static dielectric constants of the medium, respectively. For complete DR measurements of moderate to high polar solvents, $\varepsilon_\infty \approx n^2$ ($n$ being the refractive index of the medium) and $\varepsilon_s \gg \varepsilon_\infty$ and as a result, $\varepsilon_\infty$ dominates the Pekar factor. This is the reason for $\lambda_s$ to be weakly dependent on solvent polarity for the systems (normal solvents, IL and the DES) considered here.

Similar insensitivity to medium polarity is also obvious from the dynamic Stokes shift values measured in time-dependent fluorescent Stokes shift experiments employing a dipolar probe in these media. The reorganization energy is connected to dynamic Stokes shift as follows, $\lambda_s \sim \frac{1}{2}[\nu(t=0) - \nu(t=\infty)]$.[46]

**Table 5.** Comparison of multi-exponential fit parameters of analytically calculated and simulated $C_1(t)$ for deep eutectic system (DES).

| | $C_1(t)$ | Without CIM | With CIM | Available simulation results[40–42] |
|---|---|---|---|---|
| DES[40] | $\tau_{avg}$(ps) | 708.93 | 225 | 60.80 |
| IL[41] | $\tau_{avg}$(ps) | 667 | 583 | 34,830 |
| Ethanol[42] | $\tau_{avg}$(ps) | 43.45 | 30.30 | 27 |

For normal dipolar solvents,[47] BMIMBF4[48] and (acetamide+LiBr) DES[49,50] the measured dynamic Stokes shift values lie in the range, 1500–2000 $cm^{-1}$. This makes the reorganization energy comparable for these systems which renders a weak polarity dependence of reorganization energy in these media.

## 4. Conclusions

In this analytical study, we have investigated the origin behind the near-independence of rates of electron transfer reaction (ETR) in solvents of widely different viscosities. Three differently viscous media – an ionic liquid ([BMIM][$PF_6$], $\eta \sim 310$cP), a dipolar solvent (ethanol, $\eta \sim 1.09$cP) and a high viscous deep eutectic solvent (acetamide+ LiBr, $\eta \sim 1950$cP) have been chosen for the representative calculations. Rotational part of the solvent friction was calculated employing the available experimental DR data. Missing dispersion ($\varepsilon_\infty - n^2$) in the available experimental DR data have been incorporated in our calculations *via* a CIM centered at 100 $cm^{-1}$. Subsequent calculations of $\Gamma_R(\kappa \to 0, z)$ reveal that the high-frequency values of this frictional kernel are nearly identical, although their zero frequency values are very different. This insensitivity of $\Gamma_R(\kappa \to 0, z)$ in the limit of high frequency to medium viscosity can explain the near-independence and/or strong decoupling of CTR rate from medium viscosity. Calculated reorientational correlation functions for $\ell = 1$ have been found to agree better with simulation predictions after incorporating the CIM contribution to the available experimental DR data. These observations reflect the need of DR measurements in THz frequency regime.

## Supplementary Information (SI)

SI contains analytically calculated decay of reorientational time correlation function (RTCF) of rank 1 with experimentally available DR data for three studied systems (DES, IL and dipolar solvent), Comparison among tri-exponential fit parameters of RTCFs of rank 1 for these three systems with and without CIM along with available simulation results. Figures S1 and Tables S1–S3 are available at www.ias.ac.in/chemsci.

## References


1. Hynes J T 1986 Chemical reaction rates and solvent friction *J. Stat. Phys.* **42** 149
2. Bagchi B 2012 *Molecular Relaxation in Liquids* (USA: OUP) p. 312
3. Straub J E, Borkovec M and Berne B J 1986 Non-Markovian activated rate processes: comparison of current theories with numerical simulation data *J. Chem. Phys.* **84** 1788
4. Carmeli B and Nitzan A 1983 Non-Markovian theory of activated rate processes. I. Formalism *J. Chem. Phys.* **79** 393
5. Chavanis P H 2019 The generalized stochastic Smoluchowski equation *Entropy* **21** 1006
6. Smoluchowski M V 1916 Über Brownsche Molekularbewegung Unter Einwirkung Äußerer Kräfte Und Deren Zusammenhang Mit Der Verallgemeinerten Diffusionsgleichung *Ann. Phys.* **353** 1103
7. Li X, Liang M, Chakraborty A, Kondo M and Maroncelli M 2011 Solvent-controlled intramolecular electron transfer in ionic liquids *J. Phys. Chem. B* **115** 6592
8. Lynden-Bell R 2007 Does Marcus theory apply to redox processes in ionic liquids? A simulation study *Electrochem. Commun.* **9** 1857
9. Shim Y and Kim H J 2007 Free energy and dynamics of electron-transfer reactions in a room temperature ionic liquid *J. Phys. Chem. B* **111** 4510
10. Bagchi B and Biswas R 1999 Polar and nonpolar solvation dynamics, ion diffusion, and vibrational relaxation: Role of biphasic solvent response in chemical dynamics *Adv. Chem. Phys.* **109** 207
11. Bagchi B and Biswas R 1998 Ionic mobility and ultrafast solvation: control of a slow phenomenon by fast dynamics *Acc. Chem. Res.* **31** 181
12. Daschakraborty S and Biswas R 2012 Ultrafast solvation response in room temperature ionic liquids: Possible origin and importance of the collective and the nearest neighbour solvent modes *J. Chem. Phys.* **137** 114501
13. Daschakraborty S, Pal T and Biswas R 2013 Stokes shift dynamics of ionic liquids: Solute probe dependence, and effects of self-motion, dielectric relaxation frequency window, and collective intermolecular solvent modes *J. Chem. Phys.* **139** 164503
14. Kashyap H K and Biswas R 2008 Dipolar solvation dynamics in room temperature ionic liquids: An effective medium calculation using dielectric relaxation data *J. Phys. Chem. B* **112** 12431
15. González B, Calvar N, Gómez E and Domínguez Á 2007 Density, dynamic viscosity, and derived properties of binary mixtures of methanol or ethanol with water, ethyl acetate, and methyl acetate at T=(293.15, 298.15, and 303.15)K *J. Chem. Thermodyn.* **39** 1578
16. Mukherjee K, Das A, Choudhury S, Barman A and Biswas R 2015 Dielectric relaxations of (acetamide + electrolyte) deep eutectic solvents in the frequency window, $0.2 \leq \nu/\text{GHz} \leq 50$: Anion and cation dependence *J. Phys. Chem. B* **119** 8063
17. Roy S and Bagchi B 1994 Solvation dynamics, energy distribution and trapping of a light solute ion *Chem. Phys.* **183** 207
18. Roy S and Bagchi B 1993 Solvation dynamics in liquid water. A novel interplay between librational and diffusive modes *J. Chem. Phys.* **99** 9938
19. Roy S and Bagchi B 1993 Ultrafast underdamped solvation: Agreement between computer simulation and various theories of solvation dynamics *J. Chem. Phys.* **99** 1310

20. Bagchi B 1989 Dynamics of solvation and charge transfer reactions in dipolar liquids *Annu. Rev. Phys. Chem.* **40** 115
21. Bagchi B and Chandra A 1991 Collective orientational relaxation in dense dipolar liquids *Adv. Chem. Phys.* **80** 1
22. Waisman E and Lebowitz J L 1972 Mean spherical model integral equation for charged hard spheres. II. Results *J. Chem. Phys.* **56** 3093
23. Waisman E and Lebowitz J L 1972 Mean spherical model integral equation for charged hard spheres I. Method of solution *J. Chem. Phys.* **56** 3086
24. Stoppa A, Hunger J, Buchner R, Hefter G, Thoman A and Helm H 2008 Interactions and dynamics in ionic liquids *J. Phys. Chem. B* **112** 4854
25. Kindt J T and Schmuttenmaer C A 1996 Far-infrared dielectric properties of polar liquids probed by femtosecond terahertz pulse spectroscopy *J. Phys. Chem.* **100** 10373
26. Biswas R and Bagchi B 1996 Solvation dynamics in slow, viscous liquids: Application to amides *J. Phys. Chem.* **100** 1238
27. Nandi N, Roy S and Bagchi B 1995 Ultrafast solvation dynamics in water: Isotope effects and comparison with experimental results *J. Chem. Phys.* **102** 1390
28. Kashyap H K and Biswas R 2010 Stokes shift dynamics in ionic liquids: Temperature dependence *J. Phys. Chem. B* **114** 16811
29. Chakraborty A, Inagaki T, Banno M, Mochida T and Tominaga K 2011 Low-frequency spectra of metallocenium ionic liquids studied by terahertz time-domain spectroscopy *J. Phys. Chem. A* **115** 1313
30. Giraud G, Gordon C M, Dunkin I R and Wynne K 2003 The effects of anion and cation substitution on the ultrafast solvent dynamics of ionic liquids: A time-resolved optical Kerr-effect spectroscopic study *J. Chem. Phys.* **119** 464
31. Shirota H and Castner E W 2005 Physical properties and intermolecular dynamics of an ionic liquid compared with its isoelectronic neutral binary solution *J. Phys. Chem. A* **109** 9388
32. Shirota H and Castner E W 2005 Why Are viscosities lower for ionic liquids with −CH2Si(CH3)3 vs −CH2C(CH3)3 substitutions on the imidazolium cations? *J. Phys. Chem. B* **109** 21576
33. Shirota H, Nishikawa K and Ishida T 2009 Atom substitution effects of [XF6]− in ionic liquids. 1. Experimental study *J. Phys. Chem. B* **113** 9831
34. Fujisawa T, Nishikawa K and Shirota H 2009 Comparison of interionic/intermolecular vibrational dynamics between ionic liquids and concentrated electrolyte solutions *J. Chem. Phys.* **131** 244519
35. Turton D A, Hunger J, Stoppa A, Hefter G, Thoman A, Walther M, et al. 2009 Dynamics of imidazolium ionic liquids from a combined dielectric relaxation and optical Kerr effect study: Evidence for mesoscopic aggregation *J. Am. Chem. Soc.* **131** 11140
36. Shim Y and Kim H J 2008 Dielectric relaxation, ion conductivity, solvent rotation, and solvation dynamics in a room-temperature ionic liquid *J. Phys. Chem. B* **112** 11028
37. Schröder C and Steinhauser O 2009 On the dielectric conductivity of molecular ionic liquids *J. Chem. Phys.* **131** 114504
38. Schröder C, Hunger J, Stoppa A, Buchner R and Steinhauser O 2008 On the collective network of ionic liquid/water mixtures. II. Decomposition and interpretation of dielectric spectra *J. Chem. Phys.* **129** 18450
39. Biswas R, Das A and Shirota H 2014 Low-frequency collective dynamics in deep eutectic solvents of acetamide and electrolytes: A femtosecond Raman-induced Kerr effect spectroscopic study *J. Chem. Phys.* **141** 134506
40. Das S, Biswas R and Mukherjee B 2015 Orientational jumps in (acetamide+ electrolyte) deep eutectics: Anion dependence *J. Phys. Chem. B* **119** 11157
41. Pal T and Biswas R 2013 Rank-dependent orientational relaxation in an ionic liquid: An all-atom simulation study *Theor. Chem. Acc.* **132** 1348
42. Saiz L, Padró J A and Guàrdia E 1997 Structure and dynamics of liquid ethanol *J. Phys. Chem. B* **101** 78
43. Matyushov D V 2004 Solvent reorganization energy of electron-transfer reactions in polar solvents *J. Chem. Phys.* **120** 7532
44. Marcus R A 1993 Electron transfer reactions in chemistry. Theory and experiment *Rev. Mod. Phys.* **65** 599
45. Marcus R A 1956 On the theory of oxidation-reduction reactions involving electron transfer. I *J. Chem. Phys.* **24** 966
46. Biswas R, Lewis J E and Maroncelli M 1999 Electronic spectral shifts, reorganization energies, and local density augmentation of Coumarin 153 in supercritical solvents *Chem. Phys. Lett.* **310** 485
47. Horng M L, Gardecki J A, Papazyanand A and Maroncelli M 1995 Subpicosecond measurements of polar solvation dynamics: Coumarin 153 revisited *J. Phys. Chem.* **99** 17311
48. Zhang X X, Liang M, Hunger J, Buchner R and Maroncelli M 2013 Dielectric relaxation and solvation dynamics in a prototypical ionic liquid + dipolar protic liquid mixture: 1-Butyl-3-methylimidazolium tetrafluoroborate + water *J. Phys. Chem. B* **117** 15356
49. Guchhait B, Das S, Daschakraborty S and Biswas R 2014 Interaction and dynamics of (alkylamide + electrolyte) deep eutectics: Dependence on alkyl chain-length, temperature, and anion identity *J. Chem. Phys.* **140** 104514
50. Subba N, Tarif E, Sen P and Biswas R 2020 Subpicosecond solvation response and partial viscosity decoupling of solute diffusion in ionic acetamide deep eutectic solvents: Fluorescence up-conversion and fluorescence correlation spectroscopic measurements *J. Phys. Chem. B* **124** 1995